Presynaptic Calcium Dynamics and Transmitter Release Evoked by Single Action Potentials at Mammalian Central Synapses

Saurabh R. Sinha,* Ling-Gang Wu,# and Peter Saggau*
*Division of Neuroscience, Baylor College of Medicine, Houston, Texas 77030, and #Abteilung Zellphysiologie, Max-Planck Institut für medizinische Forschung, D-69120 Heidelberg, Germany

ABSTRACT The relationship between presynaptic calcium transients ($[Ca^{2+}]_t$) and transmitter release evoked by a single stimulus was both investigated experimentally and modeled at a mammalian central synapse, the CA3 to CA1 pyramidal cell synapse in guinea pig hippocampal slices. In the present study, we compared the low-affinity calcium indicator furaptra with the higher-affinity indicator fura-2. The 10–90% rise time of the furaptra transient was 2.4 ms compared to 7.8 ms with fura-2; the half-decay time ($\tau_{1/2}$) was 30 ms for furaptra, compared to 238 ms for fura-2. The half-width of the calcium influx was 1.8 ms with furaptra, which provides an upper limit to the duration of the calcium current (I_{Ca}) evoked by an action potential. Modeling the decay time course of the furaptra transients led to the conclusion that the predominant endogenous calcium buffer in these terminals must have relatively slow kinetics ($k_{on} < 10^5$/M·s), although the presence of small amounts of fast buffers cannot be excluded. The relationship between the $[Ca^{2+}]_t$ measured with furaptra and the postsynaptic response was the same as previously observed with fura-2: the postsynaptic response was proportional to about the fourth power ($m \approx 4$) of the amplitude of either $[Ca^{2+}]_t$ or calcium influx. Thus, although fura-2 may be locally saturated by the high local $[Ca^{2+}]$ responsible for transmitter release, the volume-averaged fura-2 signal accurately reflects changes in this local concentration. The result that both indicators gave similar values for the power m constrains the amplitude of calcium influx in our model: $I_{Ca} < 1$ pA for 1 ms.

INTRODUCTION

An action potential invading a presynaptic terminal opens voltage-dependent Ca^{2+} channels (VDCCs), which leads to a transient increase in presynaptic calcium concentration ($[Ca^{2+}]_t$), which then triggers neurotransmitter release. Based on the evidence that the postsynaptic response is proportional to about the third or fourth power of the extracellular $[Ca^{2+}]$ at the neuromuscular junction (Dodge and Rahamimoff, 1967) and the squid giant synapse (Katz and Miledi, 1970), it was first proposed that calcium acts in a cooperative manner to cause transmitter release. More recently, the postsynaptic response was found to be a third to fourth power function of the presynaptic I_{Ca} at the squid giant synapse (Augustine et al., 1985; Augustine and Charlton, 1986). A highly nonlinear dependence of postsynaptic response on presynaptic $[Ca^{2+}]$ was also found at the crayfish neuromuscular junction during tetanic stimulation (Zucker et al., 1991). At the same synapse, a similar relationship was found by uniformly increasing presynaptic $[Ca^{2+}]$ using photolysis of a light-sensitive calcium chelator (Landò and Zucker, 1994). This technique avoided the problems of associating the readily detectable spatially averaged $[Ca^{2+}]_t$ or I_{Ca} with the local $[Ca^{2+}]$ near the membrane, which is not detectable but is responsible for evoked release.

The development of techniques for selectively loading calcium indicators into presynaptic terminals in brain slice preparations (Regehr and Tank, 1991; Saggau et al., 1992; Wu and Saggau, 1994a) has allowed for the investigation of the relationship between presynaptic $[Ca^{2+}]_t$ and transmitter release at synapses in the mammalian central nervous system, which are too small to be studied by more direct techniques. These techniques directly measure the change in volume-averaged $[Ca^{2+}]$; thus calcium influx can be roughly approximated by the first derivative of the optically recorded presynaptic $[Ca^{2+}]_t$ (Wu and Saggau, 1994a). At CA3 to CA1 pyramidal cell synapses of guinea pig hippocampal slices, the field excitatory postsynaptic potentials (fEPSP) was found to be proportional to approximately the fourth power of the presynaptic $[Ca^{2+}]_t$ or calcium influx evoked by a single stimulus. This relationship was determined by application of several VDCC blockers such as Cd^{2+} (Wu and Saggau, 1994a), ω-conotoxin-GVIA (ω-CTx-GVIA) and ω-agatoxin-IVA (ω-ATx-IVA) (Wu and Saggau, 1994b), and ω-conotoxin-MVIIC (ω-CTx-MVIIC) (Wu and Saggau, 1995a). These studies were performed with the relatively high-affinity indicator fura-2, which has a dissociation constant (K_d) of approximately 200 nM (Kao and Tsien, 1988). Fura-2 was used because an indicator with a K_d near the resting $[Ca^{2+}]$ is ideal for measuring resting levels and gives large changes in signal for $[Ca^{2+}]_t$ starting from rest. However, it has been shown in other preparations that the local $[Ca^{2+}]$ for triggering transmitter release ranges from tens to hundreds of μM (Roberts et al., 1990; Llinás et al., 1992; Heidelberger et al., 1994). Thus the use of high-affinity indicators will result in local saturation of the recorded signal near VDCCs and transmitter release

Received for publication 8 July 1996 and in final form 13 November 1996.
Address reprint requests to Dr. Peter Saggau, Division of Neuroscience, S-603, Baylor College of Medicine, One Baylor Plaza, Houston, TX 77030. Tel.: 713-798-5082; Fax: 713-798-3946; E-mail: psaggau@bcm.tmc.edu.

0006-3495/97/02/637/15 $2.00

sites. Moreover, because of their slow kinetics, such indicators have a limited ability to follow rapid changes in $[Ca^{2+}]$ and may also significantly contribute to the calcium buffering capacity within the presynaptic terminal (Baylor and Hollingworth, 1988; Regehr and Alturi, 1995). Last, it has recently been shown that bath-applied Cd^{2+} may interfere with signals recorded by high-affinity indicators (Regehr and Alturi, 1995).

As furaptra was developed as a magnesium indicator (Raju et al., 1989), it has a relatively low affinity for calcium ($K_d \approx 50$ μM). Comparison of the $[Ca^{2+}]_t$ measured in rat cardiac myocytes with furaptra and fura-2 have shown that furaptra signals show fewer problems with local saturation, Ca^{2+} binding kinetics, and Ca^{2+} buffering than fura-2 (Berlin and Konishi, 1993). Furaptra signals also report $[Ca^{2+}]_t$ more accurately than fura-2 during stimulus trains (Regehr and Alturi, 1995). With furaptra, the relationship between presynaptic $[Ca^{2+}]_t$ and postsynaptic response was measured at the synapse between parallel fibers and Purkinje neurons in rat cerebellar slices (Mintz et al., 1995). The relationship was exponential; the exponent m was approximately 2.5 for Cd^{2+} and ω-CTx-GVIA and 4 for ω-ATx-IVA.

To address the concerns associated with fura-2 measurements, in this study we investigated the relationship between presynaptic $[Ca^{2+}]_t$ and transmitter release at the hippocampal CA3 to CA1 synapse using furaptra. During application of Cd^{2+}, the relationship was the same as we had reported previously using fura-2: approximately a fourth power. We used our measurements with fura-2 and furaptra to develop a simple model of a presynaptic nerve terminal (based on Sala and Hernandez-Cruz, 1990). The model incorporated radial diffusion of substances, endogenous and exogenous Ca^{2+} buffers, I_{Ca}, a Ca^{2+} pump, and transmitter release. Fitting model parameters to our experimental results allowed us to constrain certain model parameters that have not previously been measured directly or modeled in mammalian central nervous system (CNS) presynaptic terminals. Specifically, these parameters are the kinetics of the predominant endogenous Ca^{2+} buffers and the amplitude of I_{Ca} evoked by a single action potential. Portions of this work have appeared before in abstract form (Sinha et al., 1996).

MATERIALS AND METHODS

Brain slice preparation

Transverse hippocampal slices were prepared by standard methods from 2–4-week-old guinea pigs. The animals were anesthetized (methoxyflurane) and quickly decapitated. Brain slices were prepared from the middle third of the hippocampus on a vibrating tissue slicer (Vibratome 1000, TPI) and were stored at room temperature in artificial cerebrospinal fluid (ACSF) containing (in mM): NaCl 124, KCl 5, $CaCl_2$ 2.5, $MgCl_2$ 1.2, $NaHCO_3$ 22, D-glucose 10. The ACSF was saturated with 95% O_2/5% CO_2 to maintain a constant pH of 7.4. After a resting period of at least 1 h, the slices were transferred to a temperature-controlled (28–30°C) recording chamber.

Loading technique and recording procedure

Previously, our laboratory developed a local injection technique for selectively loading fura-2 into presynaptic terminals of hippocampal CA3 to CA1 synapses (Wu and Saggau, 1994a). In this study, we used this technique to selectively load furaptra into the same population of terminals. The membrane-permeable acetoxymethyl ester of furaptra (furaptra-AM; Molecular Probes, Eugene, OR) was prepared for injection as follows: 50 μg of furaptra-AM was dissolved in 5 μl dimethyl sulfoxide containing 10% pluronic acid, 50 μl ACSF was added, and the mixture was sonicated for at least 1 min. The final solution contained 1.4 mM furaptra-AM, 10% dimethyl sulfoxide, and 1% pluronic acid. This solution was prepared each day and was used within 1 h. A small amount of the solution ($\ll 1$ μl) was pressure-injected into the slice in stratum radiatum (SR) of area CA1. About 1 h after injection, fluorescence emerging from the recording area in SR of area CA1 was detected by a single photodiode. The recording area had a diameter of about 150 μm and was 0.5–1 mm away from the site of injection. An extracellular recording electrode (filled with 2 M NaCl, 1–5 MΩ) was placed in the center of the fluorescence recording area to record the fEPSP. Responses were evoked by a single electrical stimulus given to CA3 axons in the Schaffer collateral-commissural pathway (SCC) through a bipolar tungsten electrode positioned in SR close to the furaptra-AM injection site.

The optical recording system consisted of an inverted microscope (Axiovert 10, Zeiss) with a 50× objective (0.9 N.A., Zeiss), equipped with a xenon arc lamp (Osram), an electromechanical shutter (Uniblitz, Vincent), and a quartz illuminator. Excitation light was filtered with a 380/10-nm bandpass filter (380-nm center wavelength, 10-nm full width at half-maximum intensity); the emitted fluorescence was filtered with a 510/40-nm bandpass. To ensure that the optical signals were not significantly filtered by the characteristics of the photodiode amplifier, for most experiments we decreased the feedback resistance to 100 MΩ from 1 GΩ, which was used previously (for example, Wu and Saggau, 1994a). This reduced the time constant of the photodiode to 180 μs from 1.4 ms (data not shown). The smaller feedback resistance resulted in a noisier signal, which necessitated increased signal averaging compared to our previous studies with fura-2.

The only signals that were calibrated were the measurements of resting $[Mg^{2+}]$ and $[Ca^{2+}]$. For this, an additional excitation bandpass filter (360/10 nm) was used to obtain a ratio measurement (see Raju et al., 1989, or Grynkiewicz et al., 1985, for details on calibration). Parameters for calculating $[Mg^{2+}]$ were determined using a Mg calibration kit (Molecular Probes, Eugene, OR) to which 40 μM furaptra was added; for resting $[Ca^{2+}]$, a Ca calibration kit with 40 μM fura-2 added was used. All signals were corrected for autofluorescence of the brain slice, which was measured before the injection of furaptra-AM. After correcting for autofluorescence, all optical transients were expressed as change in fluorescence divided by resting fluorescence ($\Delta F/F$). Averaging techniques ($n \leq 60$, 10–20 s interval) were used to improve the signal-to-noise ratio. All data are expressed as mean ± SEM. To measure the relationship between presynaptic $[Ca^{2+}]_t$ (expressed as $\Delta F/F$) or calcium influx ($d(\Delta F/F)/dt$) and the fEPSP, the amplitudes of the presynaptic $[Ca^{2+}]_t$ or calcium influx and the maximal slope of the fEPSP were used. The maximum slope of the fEPSP is proportional to the amplitude of the excitatory postsynaptic current (EPSC). The degree of cooperativity (m) was determined from the best fit of the data to the equation

$$\text{fEPSP} \propto K_1([Ca^{2+}]_t)^m \approx K_2\left(\frac{\partial[Ca^{2+}]_t}{\partial t}\right)^m, \qquad (1)$$

where K_1 and K_2 are proportionality constants. The best fit was found by performing a linear regression on logarithms of the data: the slope of the linear regression equals m.

Modeling

The model we used was based on the model of calcium diffusion and buffering in a spherical neuron developed by Sala and Hernandez-Cruz

(1990). Several parameters were altered to fit the data, and functions for transmitter release and fluorescence of a calcium indicator were added. Fig. 1 shows a schematic of the model. The full model includes several diffusible species (S): Ca^{2+}, two endogenous calcium buffers (B_1 and B_2), an exogenous calcium buffer (Ind, the calcium indicator), and the Ca^{2+}-bound forms of all buffers. If only radial diffusion is considered in a spherical structure, the diffusion equation reduces to (Crank, 1978)

$$\frac{\partial r[S]}{\partial t} = D_S \frac{\partial^2 r[S]}{\partial r^2}, \qquad (2)$$

where $[S]$ is the concentration of the species at a distance r from the center of the sphere and D_S is its diffusion coefficient. D_{Ca} was 6×10^{-6}/cm^2·s; immobile species have $D_S = 0$; values for D_S and other model parameters are listed in Table 1. The value for D_{Ca} used represents free diffusion of Ca^{2+} and does not take into account the tortuosity of the compartment (Sala and Hernandez-Cruz, 1990). The tortuosity of the intracellular compartments is often taken into account by reducing D_{Ca} by a factor of 2–3; however, no direct data are available regarding the tortuosity of the presynaptic terminals being modeled. Furthermore, because of the small size of the terminal, even a 10-fold decrease in D_{Ca} (6×10^{-7}/cm^2·s) did not significantly affect the simulation results presented in this paper (data not shown). The presynaptic terminal modeled here represents the average of the thousands of terminals from which we simultaneously record during a single experiment. If this were not the case, a Monte Carlo-type simulation would be more appropriate because of the small absolute number of molecules being considered in some of the simulations; moreover, the assumption of radial symmetry would be far more questionable.

Discretization of Eq. 2 led to a model consisting of concentric spherical shells, where the concentration of all species was assumed to be uniform within a shell. Our model of a spherical presynaptic terminal of 0.5 μm radius was discretized into 10 shells, each 50 nm thick. A finite-difference approximation (first-order Euler scheme) was used to numerically solve Eq. 2 and the other differential equations given below (for more details on numerical solutions, see Sala and Hernandez-Cruz, 1990).

Initially, all species are assumed to be distributed homogeneously with known free intracellular $[Ca^{2+}]$ and known total concentrations of the buffers. The initial concentrations of free buffers and Ca^{2+}-bound buffers were calculated from the mass-action laws for each buffer based on the following first-order kinetic scheme:

$$[Ca^{2+}] + [B] \underset{k_{off}}{\overset{k_{on}}{\rightleftharpoons}} [BCa],$$

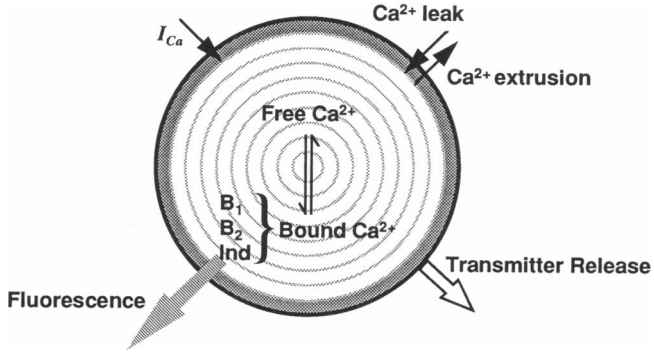

FIGURE 1 Schematic of model presynaptic terminal. The model consists of concentric spherical shells with homogeneous concentration of all species within a shell and diffusion between shells. The processes modeled in the outermost shell (*shaded*) are calcium influx (I_{Ca}), extrusion and leak, and transmitter release. Binding of calcium to three buffers is also modeled: two endogenous buffers (B_1 and B_2) and an exogenous buffer (Ind). Fluorescence emission of the calcium indicator (Ind) is also modeled.

TABLE 1 Initial values (Sala and Hernandez-Cruz, 1990) and values used (if different) in most simulations for model parameters

Parameter	Initial value	Value used
Radius		500 nm
Number of shells		10
Time step		250 ns
Calcium		
Initial free concentration	50 nM	NC
D_{Ca}	6×10^{-6} cm^2/s	NC
Fast buffer, B_1		
Total concentration	100 μM	0
K_d	1 μM	
k_{on}	10^8/M · s	
D_{B1}	5×10^{-7} cm^2/s	
Slow buffer, B_2		
Total concentration	600 μM	NC
K_d	400 nM	NC
k_{on}	5×10^5/M · s	5×10^4/M · s
D_{B2}	0 cm^2/s	NC
Indicator		
Total concentration	10 μM	NC
K_d		
Furaptra		50 μM
Fura-2	200 nM	NC
k_{on}	10^8/M · s	NC
D_{Ind}	2.5×10^{-6} cm^2/s	NC
F_{bound}/F_{free}		0.06
Calcium extrusion		
$Rate_{max}$	2 pmol/cm^2 · s	NC
K_m	830 nM	NC
Transmitter release		
K_d		100 μM
m		4
τ_{max}		100 μs

NC, No change.

where B is an endogenous or exogenous buffer (calcium indicator), BCa is the Ca^{2+}-bound buffer, and k_{on} and k_{off} are the on- and off-rate constants, respectively. The equilibrium dissociation constant (K_d) is equal to k_{off}/k_{on}. The model employed two endogenous buffers: a fast, mobile buffer with relatively low capacity (B_1) and a slow, immobile buffer with high capacity (B_2). The initial properties of these buffers were based on the work of Sala and Hernandez-Cruz (1990), who used B_1 to represent the intrinsic buffers and B_2 for the smooth endoplasmic reticulum. Their properties were altered to match the time course of the modeled fluorescence transients to the experimentally measured signals. This process is discussed further in the Results; in brief, we found that the best fit was obtained in the absence of B_1. Therefore, the fast buffer B_1 was not included in most of the simulations in this paper, i.e., $[B_1] = 0$.

Calcium current (I_{Ca}) was modeled as an increase in $[Ca^{2+}]$ in the outermost shell ($[Ca^{2+}]_{o.s.}$):

$$\frac{\partial [Ca^{2+}]_{o.s.}}{\partial t} = -\frac{I_{Ca}}{2\mathcal{F} V_{o.s.}}, \qquad (3)$$

where $\mathcal{F}$ is Faraday's constant and $V_{o.s.}$ is the volume of the outermost shell.

All plasma membrane calcium extrusion mechanisms were lumped into a single, voltage-independent system with Michaelis-Menten kinetics that operates only in the outermost shell:

$$Rate_{pump} = \frac{\partial [Ca^{2+}]_{o.s.}}{\partial t} = \frac{-Rate_{max} \cdot A}{V_{o.s.}} \cdot \frac{[Ca^{2+}]_{o.s.}}{[Ca^{2+}]_{o.s.} + K_m} \qquad (4)$$

where $Rate_{max}$ is the maximum rate of extrusion, K_m is the calcium concentration for half-maximum activation, and A is the surface area of the terminal. To maintain a constant $[Ca^{2+}]$ at rest it was necessary to compensate for the extrusion mechanisms; therefore, a constant calcium leak equal in amplitude to $Rate_{pump}$ at rest was also included in the outermost shell.

The fluorescence (F, arbitrary units) of the calcium indicator (Ind) can be calculated from the number of the free (n_{free}) and Ca^{2+}-bound (n_{bound}) molecules of buffer:

$$\frac{F}{F_{free}} = n_{free} + \frac{F_{bound}}{F_{free}} n_{bound}, \quad (5)$$

where F_{bound}/F_{free} is the ratio of the fluorescences of the Ca^{2+}-bound and free indicator. For fura-2, F_{bound}/F_{free} is 0.06 when excited with 380-nm light (Grynkiewicz et al., 1985); furaptra appears to have a similar ratio when excited at 370 nm (Konishi and Berlin, 1993). The exact value of this ratio does not affect the modeling results because all fluorescence transients are expressed as $\Delta F/F$. Because the total amount of indicator in the terminal and the volume of the terminal are constants during the simulation, volume-average concentrations can be used instead of absolute amounts of free and bound indicator.

Transmitter release (R) was modeled as a nonlinear, saturable function of $[Ca^{2+}]$ in the outermost shell of the model presynaptic terminal. The number of vesicles (N_V) available for release, i.e., those vesicles that are docked at the active zone and only require binding of calcium ions to fuse with the presynaptic membrane and release their transmitter, was assumed to be finite and not significantly replenished during the length of a typical simulation (<25 ms). Last, we modeled transmitter release as occurring with a finite rate after calcium binding ($1/\tau_{max}$):

$$\frac{\partial N_v}{\partial t} = -\frac{1}{\tau_{max}}\left(\frac{[Ca^{2+}]_{o.s.}}{[Ca^{2+}]_{o.s.} + K_d}\right)^m N_v \quad (6)$$

$$\frac{\partial R}{\partial t} \propto -\frac{\partial N_v}{\partial t}. \quad (7)$$

As before (Eq. 1), m reflects the degree of calcium cooperativity required for transmitter release: m Ca^{2+} ions must bind to m independent but equivalent binding sites with dissociation constant K_d to release a synaptic vesicle. The transmitter release process modeled represents release from a large group of simultaneously activated presynaptic terminals, which reflects the situation in our experiment. It does not directly represent transmitter release from a single terminal. The metric used for modeled transmitter release was the maximum instantaneous release. As mentioned previously, the slope of the fEPSP, which was the metric of transmitter release used in our experiments, is proportional to the amplitude of the EPSC. Assuming that the EPSC shape is a filtered version of the time course of neurotransmitter release, the peak of the EPSC should, to a first approximation, be proportional to the maximum instantaneous release. This is of course complicated by diffusion and clearance of neurotransmitter in the synaptic cleft and the kinetics of the postsynaptic transmitter receptor (Clements et al., 1992).

RESULTS

Selective loading of furaptra into presynaptic structures

Furaptra-AM was injected into hippocampal slices as described above. Furaptra signals and fEPSPs evoked by a single electrical stimulus of the SCC pathway were simultaneously recorded in SR of area CA1. To verify that the observed furaptra signals were of presynaptic origin, the ionotropic glutamate receptor antagonists 6-cyano-7-nitroquinoxaline-2,3-dione (CNQX, 10 μM) and D-2-amino-5-phosphonopentanoic acid (D-APV, 50 μM) were applied at the end of each experiment. As found previously with fura-2-AM (Wu and Saggau, 1994a), this completely blocked the postsynaptic response to the stimulation without significantly changing the furaptra signals or the presynaptic fiber volley (Fig. 2). The facts that the onset of the furaptra transient corresponded to that of the presynaptic fiber volley and that the peak of the furaptra signal occurred well before the peak of the fEPSP also suggest a presynaptic origin.

We tested whether magnesium influx contributed to the furaptra signals because furaptra was originally designed as an indicator for intracellular Mg^{2+} (Raju et al., 1989), although we are not aware of any evidence for rapid changes (within several milliseconds) in intracellular $[Mg^{2+}]$. Application of magnesium-free solution for about 30 min enhanced the fEPSP 3.69 $\pm$ 1.16 times and the presynaptic $[Ca^{2+}]_t$ 1.44 $\pm$ 0.11 times their values in normal saline (Fig. 3 *A*). Fitting these data with Eq. 1 gives m = 3.6, consistent with the approximately fourth-power function between the fEPSP and the presynaptic $[Ca^{2+}]_t$ found by applying various VDCC blockers (Wu and Saggau, 1994a,b, 1995a). Application of calcium-free solution for about 50 min abolished synaptic transmission and the furaptra signal (Fig. 3 *B*). These results suggest that the furaptra signal reflects changes in intracellular $[Ca^{2+}]$ and not $[Mg^{2+}]$.

Because the resting $[Ca^{2+}]$ in mammalian presynaptic terminals is about 50–200 nM (Regehr and Tank, 1991; Wu and Saggau, 1994a), which is much lower than the K_d of furaptra for Ca^{2+} (50 μM), a ratio measurement of furaptra fluorescence at rest can be used to estimate $[Mg^{2+}]$ in presynaptic terminals. Based on an in vitro calibration of furaptra signals excited at 360/380 nm, the resting $[Mg^{2+}]$ in presynaptic terminals and axons of area CA3 pyramidal cells was 500 $\pm$ 200 μM (n = 6).

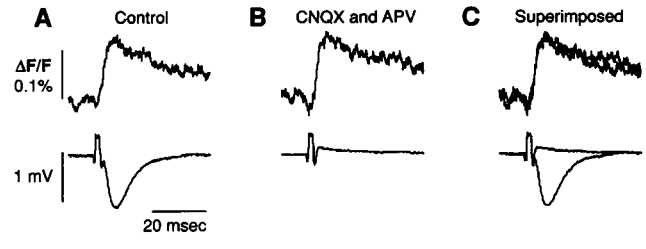

FIGURE 2 Presynaptic origin of furaptra signals. (*A*) The furaptra signal and the corresponding fEPSP (*lower panel*) evoked by a single electrical stimulus of the SCC pathway were recorded in stratum radiatum of area CA1. (*B*) Bath application of 10 μM CNQX and 50 μM D-APV abolished the fEPSP without affecting the furaptra signal or the presynaptic fiber volley. (*C*) The responses from *A* and *B* are superimposed. Furaptra signals were recorded with the slower photodiode (see Materials and Methods).

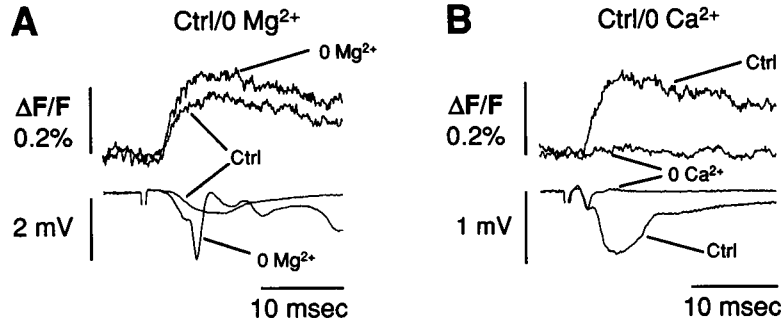

FIGURE 3 The furaptra signal reflects the Ca^{2+} transient. (*A*) Furaptra signals (*upper trace*) and fEPSPs (*lower trace*) recorded in control (Ctrl) and 30 min after application of Mg^{2+}-free ACSF. Mg^{2+}-free ACSF enhanced both the furaptra signal and the fEPSP. (*B*) Furaptra signals and fEPSPs in control and 50 min after application of Ca^{2+}-free ACSF (no added Ca^{2+}). Ca^{2+}-free ACSF essentially abolished both the furaptra signal and the fEPSP. Furaptra signals were recorded with the slower photodiode (see Materials and Methods).

Time courses of the presynaptic $[Ca^{2+}]_t$ and calcium influx

As found previously with fura-2-AM (Wu and Saggau, 1994a), injection of furaptra-AM did not change the amplitude and/or the slope of the fEPSP. This suggests that furaptra did not significantly interfere with the presynaptic $[Ca^{2+}]_t$. This is not surprising because, assuming similar concentrations for both indicators within the presynaptic terminals, a low-affinity calcium indicator should affect the presynaptic $[Ca^{2+}]_t$ much less than a higher-affinity indicator (fura-2). Fig. 4 shows the time courses of the presynaptic $[Ca^{2+}]_t$ and calcium influx measured with either furaptra or fura-2 from typical experiments. To facilitate comparison, the onsets of the transients were aligned and the amplitudes were normalized. The rising phase of the presynaptic $[Ca^{2+}]_t$ was significantly faster with furaptra compared to fura-2 ($p < 0.01$, *t*-test): the 10–90% rise time with furaptra was 2.4 ± 0.2 ms ($n = 11$), compared to 7.8 ± 0.2 ms ($n = 4$) with fura-2. The decay phase of the transients recorded with furaptra lasted about 1–3 s with a half-decay time, the time required for the transient to decay to half its peak values from its peak ($\tau_{1/2}$) of 30 ± 3 ms ($n = 5$); with fura-2 the decay phase lasted about 3–5 s, and the half-decay time was 238 ± 18 ms ($n = 8$; Wu and Saggau, 1994a). The half-decay time of the fura-2 transient was measured with the slower photodiode amplifier ($\tau = 1.4$ ms); however, this should not affect the time course of such a slow signal.

Assuming that the optically recorded signals are proportional to the volume-averaged calcium concentration, the first time derivative of the presynaptic $[Ca^{2+}]_t$ ($d(\Delta F/F)/dt$) approximates the presynaptic calcium influx after an action potential (Fig. 4 *B*). This is only an approximation because it ignores the effects of endogenous buffers; calcium clearing/extrusion mechanisms should not be a factor, as they operate on a much slower time scale. With furaptra, the half-width of the calcium influx (the time difference between the points where the transient was half its peak value on its rising and falling phases) was 1.8 ± 0.1 ms ($n = 11$), which was significantly shorter ($p < 0.01$, *t*-test) than the half-width measured with fura-2, 4.4 ± 0.2 ms ($n = 4$).

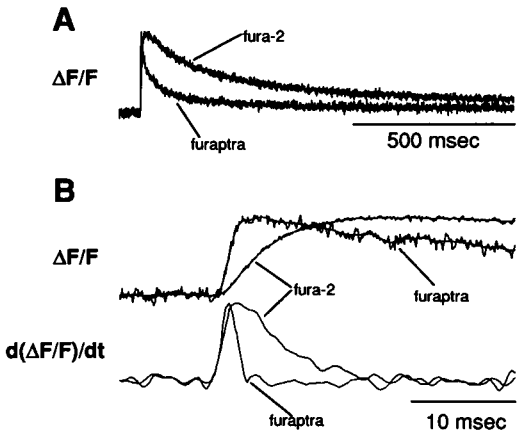

FIGURE 4 Comparison of kinetics of furaptra and fura-2 transients. (*A*) Time courses of the presynaptic $[Ca^{2+}]_t$ recorded with furaptra and fura-2 from different slices. The $[Ca^{2+}]_t$ was evoked by a single stimulation of the SCC pathway. The onsets of both transients were aligned and the amplitudes were normalized. (*B*) The presynaptic $[Ca^{2+}]_t$ (*upper trace*) and its corresponding calcium influx recorded with furaptra and fura-2 are plotted at a faster time scale. The presynaptic $[Ca^{2+}]_t$ was first smoothed (*smooth lines in upper panel*) and then numerically differentiated to obtain the calcium influx.

Modeling of the time course of furaptra transients

We used the $\tau_{1/2}$ of the furaptra transients to adjust the parameters of the endogenous buffers. Unlike the 10–90% rise time and the half-width of the calcium influx, $\tau_{1/2}$ is relatively independent of the duration of I_{Ca}, which is much shorter than $\tau_{1/2}$. Because of furaptra's lower affinity for Ca^{2+}, its kinetic parameters (K_d and rate constants) and concentration have much less effect on the time course of the calcium signal and on the time course of the actual intracellular $[Ca^{2+}]_t$ compared to fura-2 (see also Fig. 7). Therefore, fitting endogenous buffer parameters to match the time course of the furaptra transients will be relatively independent of the parameters used for furaptra (see also Fig. 5 *B*). Fig. 5 *A* shows the modeling results for the effect of varying endogenous buffer parameters on $\tau_{1/2}$. All parameters except for the endogenous buffers were as in Table 1 ("initial values"). For the endogenous buffers, we started with the same parameters as used by Sala and Hernandez-Cruz (1990): the fast buffer B_1 ($[B_1] = 100$ μM, $K_d = 1$ μM, $k_{on} = 10^8$/M·s) and the slow buffer B_2 ($[B_2] = 600$ μM, $K_d = 400$ nM, $k_{on} = 5 \times 10^5$/M·s). This resulted in a

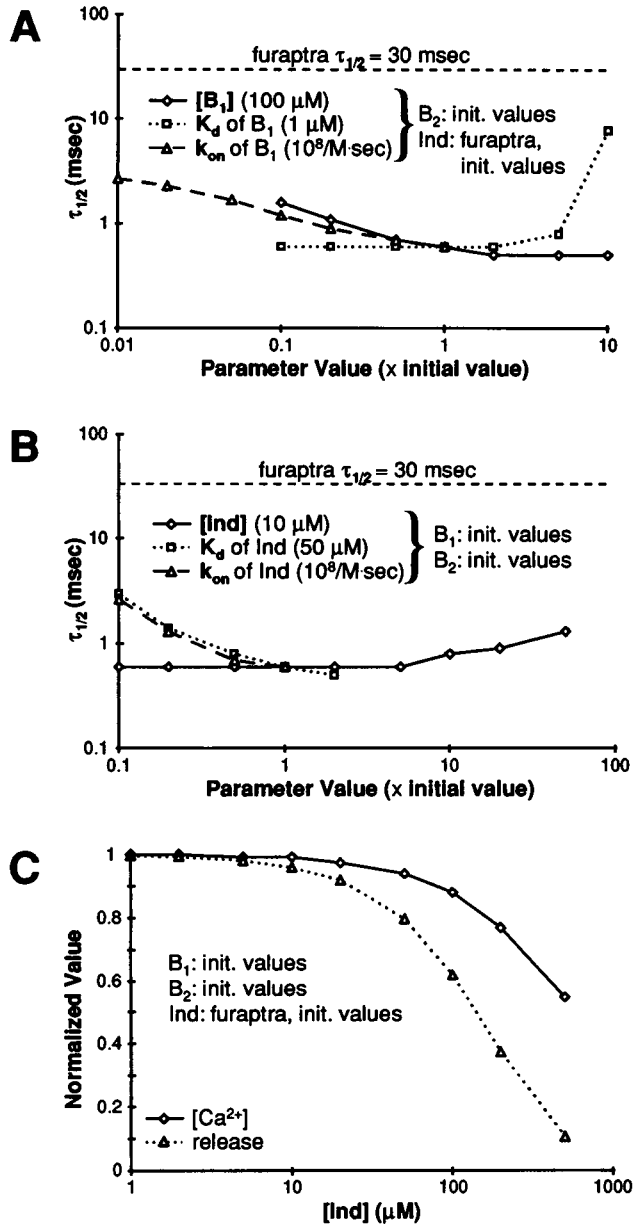

FIGURE 5 Effect of the fast buffer (B_1) and Ind parameters on $\tau_{1/2}$ of furaptra transients. (*A*) B_1 parameters (concentration, K_d, or k_{on}) were changed while keeping all other parameters equal to their initial values. The indicator modeled was one with furaptra characteristics. The half-decay times measured for furaptra transients evoked by an I_{Ca} of 1 pA for 1 ms are shown. The abscissa shows the value of the parameter being varied relative to its initial value. (*B*) Ind parameters were changed while keeping all other parameters equal to their initial values (both B_1 and B_2 are present). (*C*) The effect of changing furaptra concentration (1–500 μM) on peak volume-averaged [Ca^{2+}] and neurotransmitter release. All other parameters were set to their initial values. All values are normalized to the condition where no indicator was present.

$\tau_{1/2}$ of only 600 μs. Changing [B_1] by an order of magnitude in either direction (10 μM ≤ [B_1] ≤ 1 mM) had little effect on $\tau_{1/2}$. Similarly, changing the K_d of B_1 also had little effect, except at very large values (K_d > 25 μM). At these higher K_d's, the fast buffer prolongs the calcium transient by serving as a reservoir for Ca^{2+}: it binds calcium very quickly and then slowly releases it. These large values are well out of the range estimated indirectly by several investigators for the fast endogenous buffer in various preparations (see Discussion); therefore, it seems unlikely that the K_d of the fast buffer is as large as would be necessary to match the time course of the furaptra transient. The parameter of B_1 that had the largest effect on $\tau_{1/2}$ was its k_{on}. We only considered decreases in k_{on} because the initial value (k_{on} = 10^8/M·s) is near the diffusion limit. Decreasing the on rate 100-fold to k_{on} = 10^6/M·s only increased $\tau_{1/2}$ to 2.7 ms. Changing the diffusion coefficient of all species in the model including the buffer B_1 had little effect, because in a structure of this size the time course of diffusion is much shorter than $\tau_{1/2}$ (data not shown).

Fig. 5 *B* shows the effect of varying the parameters for the indicator while keeping the endogenous buffer parameters set to their initial value. Changing the concentration of the indicator had little effect on $\tau_{1/2}$; even at [Ind] = 500 μM, $\tau_{1/2}$ only increased to 1.3 ms, compared to 600 μs for [Ind] = 10 μM. Although we have no direct estimate of the [Ind] in our experiments, it is unlikely to be more than a few μM for several reasons: the distance between the injection and recording sites, the general divergence of axons, the fact that not all of the injected dye will be taken up and cleaved by intracellular esterases, and the small amount of dye solution injected into the slice (≪1 μl). Another reason for assuming the [Ind] to be relatively small is that synaptic transmission was not significantly altered by the presence of fura-2 or furaptra. Fig. 5 *C* shows the effects of [Ind] on the amplitude of the presynaptic calcium transient and transmitter release in the model. We consider the concentration required to cause a 10% decrease in transmitter release to be an upper limit, which is approximately 20 μM for an indicator with characteristics of furaptra and with endogenous buffer parameters set to their initial values.

We also considered the effect of changing indicator K_d. As expected, based on the slower time course of our fura-2 signals and the expected effect of indicator K_d on the time course (Regehr and Alturi, 1995), decreasing K_d increases $\tau_{1/2}$. Even in the extreme, the K_d of furaptra in the presynaptic terminals is not likely to be off by more than a factor of 2. Decreasing the indicator's k_{on} also increases $\tau_{1/2}$. Baylor and Hollingworth (1988) reported that the k_{on} for fura-2 is reduced by a factor of 6–60 in frog muscle fibers because of binding of the indicator to cytoplasmic constituents; however, this effect was not seen for exogenous buffers at the squid giant synapse (Adler et al., 1991). In the absence of such evidence, we used an intermediate value for k_{on} of 10^8/M·s for the indicators, which is sixfold lower than the value reported in cuvette measurements for fura-2 (Kao and Tsien, 1988).

From Fig. 5 it is apparent that the time course of the experimental furaptra signals cannot be matched, even with relatively large variations of B_1 or indicator parameters. The only parameter sets that even came close were those that effectively removed B_1 from playing a role in shaping the

$[Ca^{2+}]_t$; therefore, we next considered the possibility of having only the slow endogenous buffer, B_2, present. Fig. 6 *A* shows the effect of varying properties of the slow buffer ($[B_2]$, K_d and k_{on}) on $\tau_{1/2}$ in the absence of B_1. Changing the K_d had little effect. Decreasing $[B_2]$ increased $\tau_{1/2}$, with a 10-fold decrease relative to "initial values" giving a value of 21.3 ms. However, $[B_2]$ is unlikely to be this low because changing either the K_d or the concentration of the endogenous buffer would have a significant effect on the differential calcium-binding ratio (κ_B) of the buffer (Neher, 1995):

$$\kappa_B = \frac{\partial[BCa]}{\partial[Ca^{2+}]} = \frac{K_d[B]_{total}}{(K_d + [Ca^{2+}])^2}, \quad (8)$$

where $[B]_{total}$ is the total concentration of the buffer, K_d is its dissociation constant, and $[Ca^{2+}]$ refers to the resting calcium concentration. $1/\kappa_B$ gives the fraction of calcium influx that would end up as free calcium. Although κ_B has not been estimated in mammalian presynaptic terminals, in somata of mammalian neurons it is estimated to be between 100 and >1000 (for a review, see Neher, 1995). It should be noted that the concept of κ_B assumes that the binding of calcium to the buffer(s) in question is almost instantaneous; therefore, for a slow buffer, such as B_2, the actual buffering will be smaller than indicated by Eq. 8. With the initial values of the slow buffer B_2 (K_d = 400 nM, $[B_2]$ = 600 μM), the differential calcium-binding ratio was κ_B = 533; decreasing the $[B_2]$ 10-fold would reduce it to an unlikely value of κ_B = 53.3. The last parameter, the k_{on} of B_2, had a large effect on $\tau_{1/2}$ and is likely to have the largest error because of the difficulty in determining it experimentally. For $k_{on} = 5 \times 10^4$/M·s, $\tau_{1/2}$ was 20.9 ms; for $k_{on} = 2 \times 10^4$/M·s, it was 33.0 ms. The effects of changing indicator parameters on $\tau_{1/2}$ when only B_2 is present are shown in Fig. 6 *B*. As in Fig. 5 *B*, the effects are relatively small in the range of likely values for indicator parameters. Fig. 6 *C* shows the effect of [Ind] on the amplitude of the presynaptic $[Ca^{2+}]$ and transmitter release when only the slow endogenous buffer is present. In this case, even 2 μM of an indicator with furaptra's characteristics is sufficient to reduce transmitter release by 10%. The effect of an indicator with fura-2 characteristics would be even larger than those shown in Figs. 5 *C* and 6 *C*; therefore, we consider 10 μM to be an extreme upper limit for the indicator concentration in the presynaptic terminals.

Based on the above considerations, most of the subsequent simulations in this paper were performed with only one endogenous buffer, the slow buffer B_2. The only change in B_2 parameters was to reduce its k_{on} 10-fold to 5×10^4/M·s. The indicator parameters used were the same as those used by Sala and Hernandez-Cruz (1990). However, alternative parameter values were considered and are discussed whenever a result is particularly sensitive to a parameter. Fig. 7 shows the actual transients produced by the model for these parameter values and for some of the other situations in Figs. 5 and 6. Furthermore, Fig. 7 also shows the results produced when the indicator modeled was fura-2. From these transients it is apparent that furaptra is better suited to follow the true time course of changes in $[Ca^{2+}]$ and that it has a much smaller effect on this time course than fura-2.

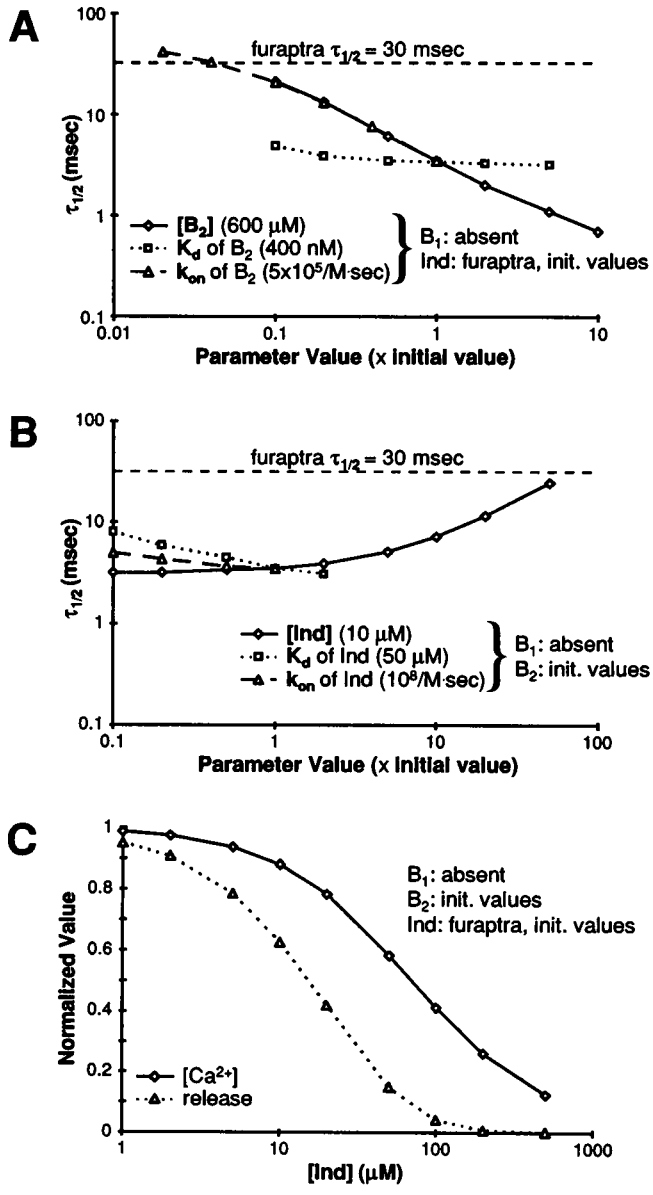

FIGURE 6 Effect of slow buffer (B_2) and Ind parameters on $\tau_{1/2}$ of furaptra transients in the absence of B_1. (*A*) B_2 parameters were changed while keeping all other parameters equal to their initial values, except for the absence of B_1. Furaptra transients were in response to an I_{Ca} of 1 pA for 1 ms. (*B*) Ind parameters were changed in the absence of B_1, with all other parameters set to their initial values. (*C*) The effect of changing furaptra concentration on the peak volume-averaged $[Ca^{2+}]$ and release. All values are normalized to the condition where no indicator was present.

Power function between the fEPSP and the presynaptic $[Ca^{2+}]_t$

Using fura-2 in CA3 to CA1 presynaptic terminals, we previously found that the amplitude of the presynaptic

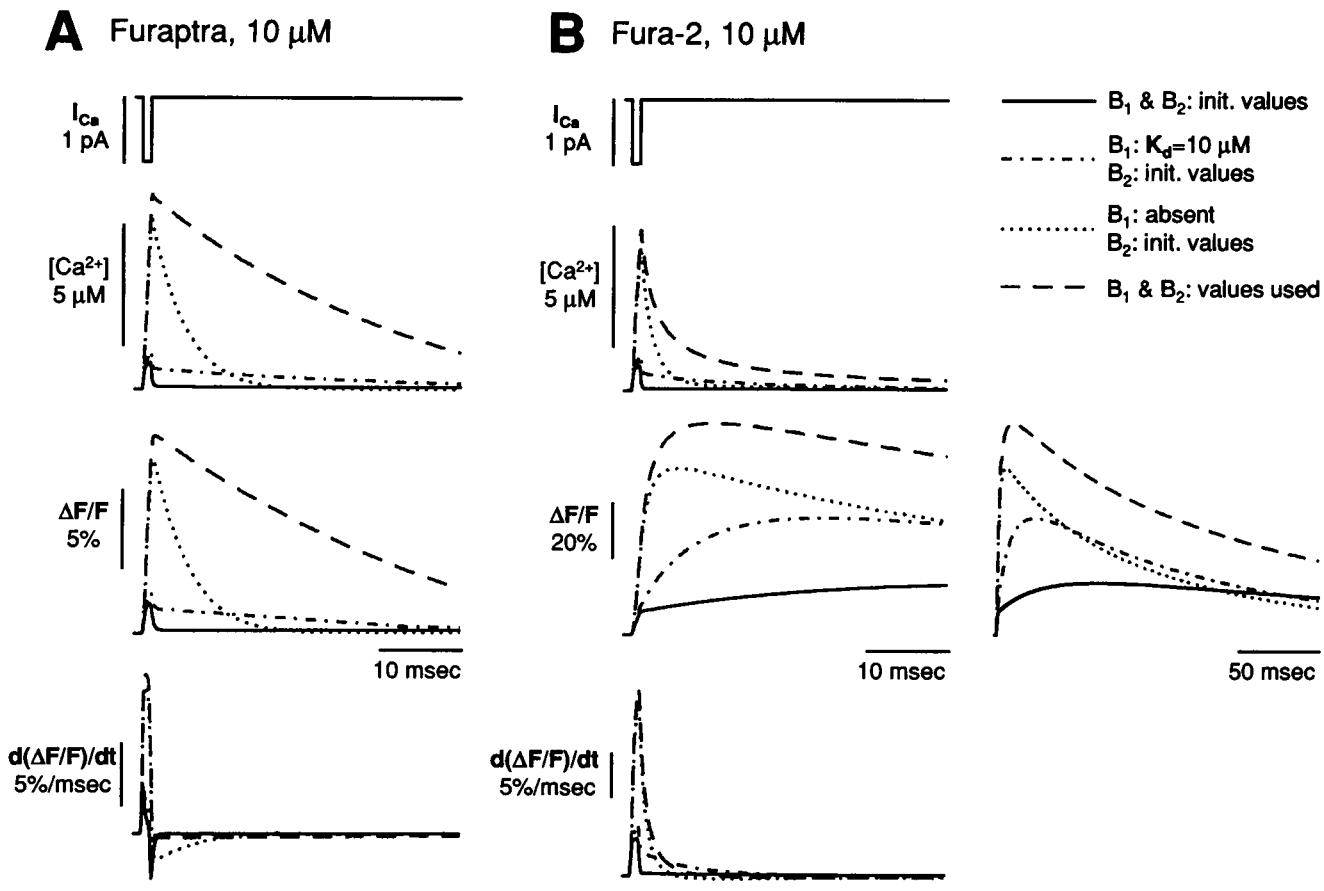

FIGURE 7 Effect of endogenous buffering parameters on model results. (*A*) Results with furaptra (10 μM) as the calcium indicator. The actual volume-averaged $[Ca^{2+}]$, fluorescence transient ($\Delta F/F$) and calcium influx ($d(\Delta F/F)/dt$) are shown for four sets of endogenous buffer parameters: 1) "initial values" from Table 1; 2) initial values, except that the dissociation constant of B_1 is increased 10-fold; 3) B_1 absent, B_2 present at "initial values"; and 4) "values used" from Table 1. For all simulations I_{Ca} = 1 pA for 1 ms. (*B*) Results with fura-2 (10 μM). The fluorescence transients are shown at a slower time scale at the right.

$[Ca^{2+}]_t$ and the volume-averaged presynaptic calcium influx were linearly related, and the fEPSP was proportional to approximately the fourth power of the presynaptic $[Ca^{2+}]_t$ or calcium influx (Wu and Saggau, 1994a). We reexamined this relationship in the present study, with furaptra as the calcium indicator. Application of the nonspecific VDCC blocker Cd^{2+} (50 μM-1 mM) reduced the presynaptic $[Ca^{2+}]_t$, calcium influx, and the fEPSP in a dose-dependent manner, without significantly changing the shape of the furaptra transients (10–90% rise time, half-width of calcium influx, $\tau_{1/2}$). Sample recordings for the application of 100 μM Cd^{2+} are shown in Fig. 8.

The relationship between the normalized amplitudes of the calcium influx and the presynaptic $[Ca^{2+}]_t$ during the application of Cd^{2+} was well fitted by a regression line with slope 0.83 $\pm$ 0.09 (r^2 = 0.90 $\pm$ 0.05, n = 3), where presynaptic $[Ca^{2+}]_t$ was the independent parameter. Thus, as shown previously with fura-2 (Wu and Saggau, 1994a), the amplitude of the presynaptic $[Ca^{2+}]_t$ can be used to estimate the volume-averaged calcium influx evoked by a single action potential. Fig. 9 *A* shows a typical example from one slice. The relationship between the slope of the fEPSP and the amplitude of the presynaptic $[Ca^{2+}]_t$ was fit to Eq. 1; the mean value for m was 3.9 $\pm$ 0.3 (n = 5). Using the volume-averaged calcium influx, the power m was determined to be 3.8 $\pm$ 0.5 (n = 3); Fig. 9, *B* and *C*, shows these relationships for a typical experiment.

Modeling of fura-2 capability of measuring power function

The fact that furaptra and fura-2 gave similar values for the power m implies that the fura-2 signal is proportional to the local calcium concentration at the release site. This must be true, even though fura-2 may be locally saturated near the cell membrane, particularly near calcium channels. Thus, although fura-2 could not be used to determine the actual calcium concentration required for transmitter release, changes in fura-2 signals are proportional to this concentration. For a large enough I_{Ca}, fura-2 will saturate throughout the terminal and would not be useful for determining m. Modeling of this phenomenon is shown in Fig. 10. Peak transmitter release is plotted against the amplitude of the calculated $[Ca^{2+}]$ and fura-2 or furaptra transients for a

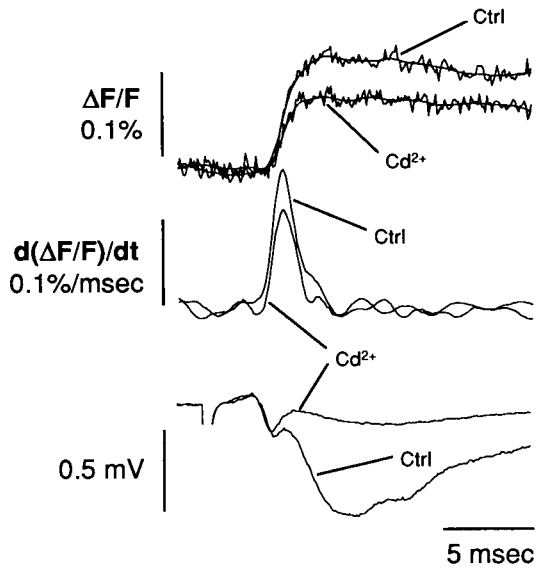

FIGURE 8 Cd^{2+} attenuates the presynaptic $[Ca^{2+}]_t$ and calcium influx without significantly changing their time course. Sample recordings of the presynaptic $[Ca^{2+}]_t$ (*top trace*), the volume-averaged calcium influx (*middle trace*), and the fEPSP (*bottom trace*) before (Ctrl) and 15 min after the application of 100 μM Cd^{2+}.

range of I_{Ca} amplitudes. For a calcium current smaller than 1 pA, both indicators give values for m near 4; note that in the model, m has been set to 4, and our interest is in the ability of fura-2 and furaptra to measure this parameter. For currents larger than 1 pA, furaptra still gives a value near 4. However, because of saturation, fura-2 now gives an extremely high and incorrect value (m = 28.7 for I_{Ca} = 1–5 pA). In combination with our experimental results, this suggests that the I_{Ca} evoked by a single action potential in a presynaptic terminal is less than 1 pA for 1 ms.

The point at which indicator saturation occurs depends on the parameters used for fura-2. This is shown in Fig. 11, where the amplitude of the fluorescence transient as a function of I_{Ca} is plotted for various sets of parameters. The effect of the dissociation constant K_d can be seen by comparing the transients for the same concentrations of fura-2 and furaptra. Even with its 250-fold higher K_d, furaptra approaches saturation for $I_{Ca} > 10$ pA. Thus small changes in the K_d of fura-2 will not significantly affect the point of saturation. The effect of changing fura-2 concentration is also shown in Fig. 11. For 2 μM fura-2, saturation occurred between 200 and 500 fA; for 50 μM fura-2, this happened near 5 pA. As discussed previously, the actual indicator concentration is not known, but we estimate it to be below 10 μM. Decreasing the k_{on} of fura-2 increases the I_{Ca} required for saturation; however, this is only a small effect, as a 10-fold decrease in k_{on} only increased the saturating I_{Ca} by approximately 2-fold. Increasing k_{on} has the effect of reducing the saturating I_{Ca} by a small amount (data not shown). Even when initial values for endogenous buffering parameters (Table 1) with 10 μM fura-2 are used, saturation still occurs at approximately 5 pA (Fig. 11). This value provides an upper estimate for I_{Ca}, as our modeling results indicate that the quantity of fast buffer, if present, is much smaller than these values. Based on the above modeling results, it appears highly unlikely that the I_{Ca} evoked by a single action potential in a presynaptic terminal is larger than 1 pA for 1 ms.

DISCUSSION

A rapid presynaptic $[Ca^{2+}]_t$ evoked by a single stimulus was recorded at hippocampal CA3 to CA1 synapses using

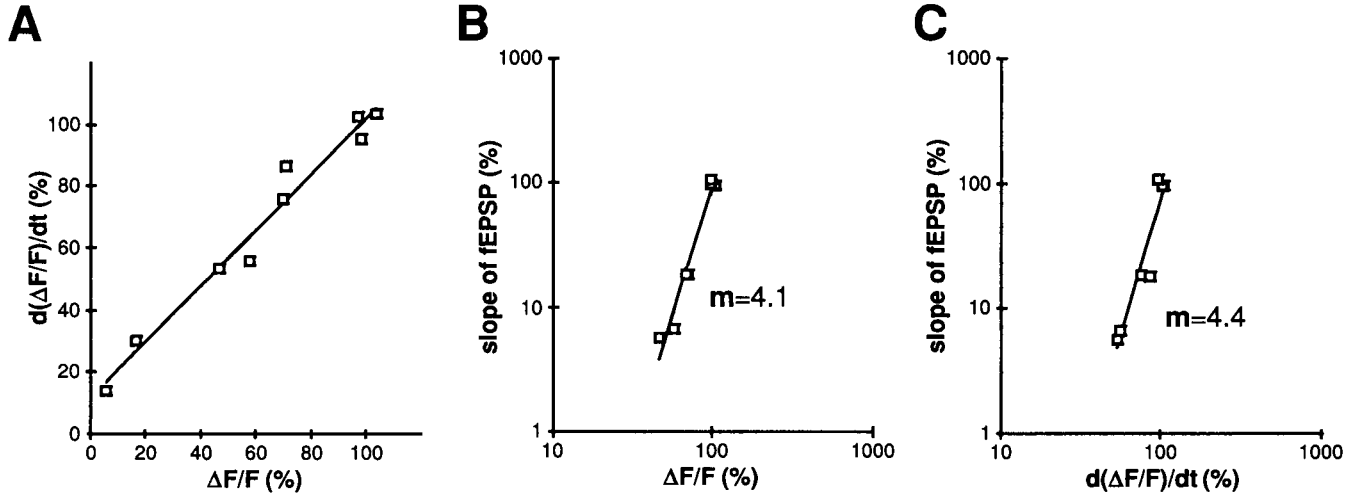

FIGURE 9 The relationship between the presynaptic $[Ca^{2+}]_t$ ($\Delta F/F$), the calcium influx ($d(\Delta F/F)/dt$), and fEPSP during application of Cd^{2+}. All data in this figure are from a single experiment; data were recorded during the sequential application of 50, 100, 200, and 1000 μM Cd^{2+}. All data were normalized to the baseline value before Cd^{2+} application. (*A*) The relationship between the amplitudes of the calcium influx and the presynaptic $[Ca^{2+}]_t$. The line shown is a fitted line (r^2 = 0.94). (*B*) The relationship between the initial slope of the fEPSP and the amplitude of the presynaptic $[Ca^{2+}]_t$ plotted on a logarithmic scale. The line was fitted using Eq. 1 (m = 4.1, r^2 = 0.98). (*C*) The relationship between the fEPSP and the amplitude of the calcium influx plotted on a logarithmic scale. The line was fitted using Eq. 1 (m = 4.4, r^2 = 0.94).

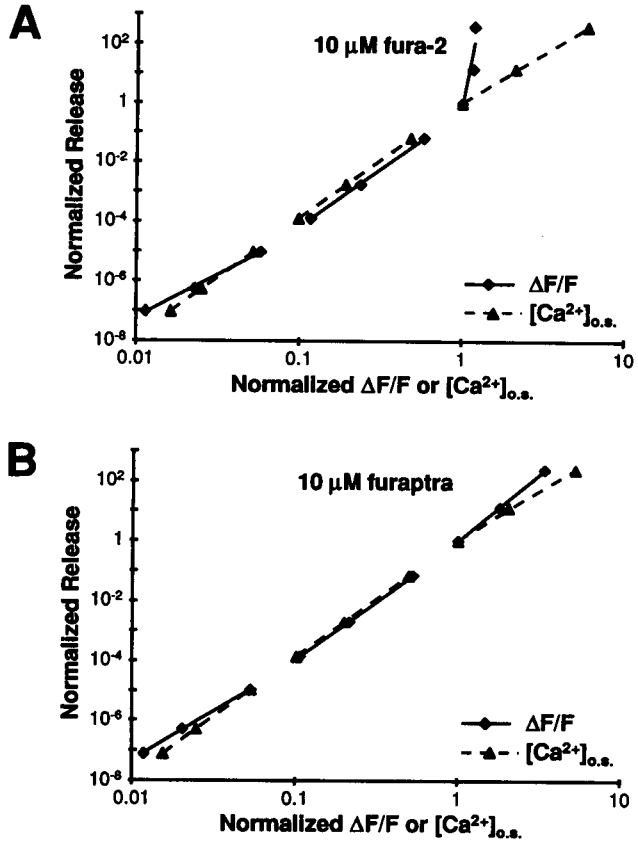

FIGURE 10 Modeling of relationship between transmitter release and amplitude of indicator transients or the $[Ca^{2+}]$ in the outermost shell ($[Ca^{2+}]_{o.s.}$). Model parameters were those labeled as "value used" in Table 1. The amplitude of I_{Ca} was varied from 10 fA to 5 pA (10, 20, 50, 100, 200, and 500 fA and 1, 2, and 5 pA); the duration was 1 ms. All data are normalized to values for 1 pA. (*A*) Results for 10 μM fura-2 are shown. The lines shown are fits. For $\Delta F/F$, the values for m of the fitted lines are 2.9 (10–50 fA), 3.9 (100–500 fA), and 28.7 (1–5 pA); for $[Ca^{2+}]_{o.s.}$, these values are 4.0, 3.9, and 3.3, respectively. (*B*) Results for 10 μM furaptra are shown. For $\Delta F/F$ the values for m of the fitted lines are 3.3 (10–50 fA), 3.9 (100–500 fA), and 4.5 (1–5 pA); for $[Ca^{2+}]_{o.s.}$, these values are 4.0, 3.9, and 3.3, respectively.

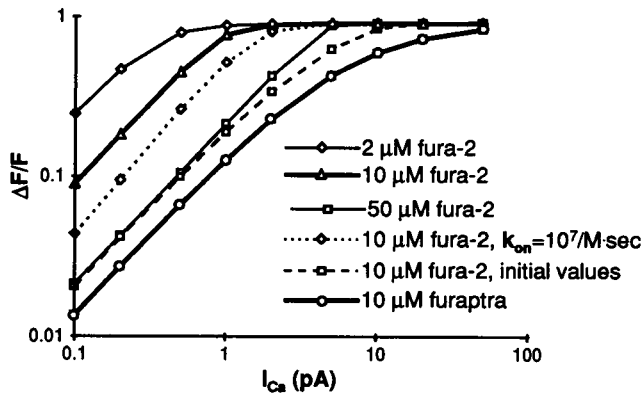

FIGURE 11 Modeling of saturation of presynaptic $[Ca^{2+}]_t$ signals. The amplitude of the fluorescence transient ($\Delta F/F$) is plotted for a range of I_{Ca} (100 fA-50 pA, duration = 1 ms) for various conditions. Fura-2 (10 μM) and furaptra (10 μM) correspond to the results shown in Fig. 10, *A* and *B*, respectively; all parameters are set to "values used" in Table 1. Results are also shown for simulations with 2 and 50 μM fura-2, with 10 μM fura-2, but with k_{on} reduced to 10^7/M·s, and with 10 μM fura-2 with parameters set to "initial values" from Table 1.

the low-affinity calcium indicator furaptra. The time course of these transients was much faster than those recorded at this synapse with the high-affinity indicator fura-2. The time course of the furaptra transients is an upper limit for that of the local $[Ca^{2+}]$ triggering transmitter release. We used the decay of the furaptra transients to constrain parameters in a simple model of a presynaptic terminal. This procedure indicated that the predominant endogenous calcium buffer in these terminals is likely to be a relatively slow buffer. By application of the nonselective VDCC blocker Cd^{2+}, we determined the relationships between the presynaptic $[Ca^{2+}]_t$ or calcium influx and transmitter release. Both relationships could be fitted by a power law with an exponent of $m \approx 4$, as we had determined previously using fura-2. The fact that furaptra and fura-2 gave approximately the same value for m indicates that the volume-averaged signal measured by fura-2 accurately represents changes in the local $[Ca^{2+}]$ responsible for triggering transmitter release, even though fura-2 is likely to be saturated by extremely high local concentrations. These data were used to further constrain parameters in the model presynaptic terminal: the amplitude and duration of I_{Ca} must be small enough that the volume-averaged fura-2 signal can be used to determine the relationship between calcium and transmitter release.

Furaptra signals represent presynaptic calcium signals

Two lines of evidence suggest that the detected furaptra signals were presynaptic. First, the furaptra transient was not sensitive to ionotropic glutamate receptor antagonists that blocked synaptic transmission (Fig. 2). Second, the onset of the furaptra transient was delayed by less than 1 ms compared to the presynaptic fiber volley, and the furaptra transient had reached its peak well before the fEPSP had reached its peak (Fig. 4). Although furaptra is sensitive to both Ca^{2+} and Mg^{2+}, the furaptra transients we recorded reflect calcium rather than magnesium influx. They were essentially abolished by applying calcium-free ACSF or high concentrations (>1 mM) of Cd^{2+}, but were enhanced by applying magnesium-free ACSF. The resting $[Mg^{2+}]$ in the presynaptic terminals was estimated to be about 500 μM (Fig. 3). During the calcium transient, Mg^{2+} bound to furaptra may be replaced by Ca^{2+}, leading to a $[Mg^{2+}]$ transient secondary to the calcium influx. However, simulations showed that this secondary transient is too slow and small to affect the rising phase of the $[Ca^{2+}]_t$, but may slightly retard the decay phase of the furaptra transient (Konishi and Berlin, 1993). Therefore, the decay phase of the actual presynaptic $[Ca^{2+}]_t$ may be slightly faster than the furaptra transient.

Comparison of furaptra and fura-2 signals

With fura-2, the presynaptic $[Ca^{2+}]_t$ evoked by a single stimulus rises to its peak within 8–12 ms at the hippocampal CA3 to CA1 synapses (Fig. 4; Wu and Saggau, 1994a) and decays to resting levels within 3–6 s at hippocampal mossy fiber to CA3 (Regehr et al., 1994) and CA3 to CA1 synapses with a $\tau_{1/2}$ of about 240 ms (Wu and Saggau, 1994a). In this study, the furaptra transients evoked by a single stimulus rose to the peak within 2–3 ms and decayed to resting levels in 1–3 s with a $\tau_{1/2}$ of approximately 30 ms (Fig. 4). The faster time course of the furaptra signals relative to fura-2 can be explained based on its lower affinity for Ca^{2+} (Regehr and Alturi, 1995). The K_d of furaptra for Ca^{2+} is approximately 50 μM in vitro (Konishi and Berlin, 1993), whereas the K_d of fura-2 is 200 nM (Kao and Tsien, 1988). The two indicators have similar on rates; therefore, the k_{off} of furaptra is more than an order of magnitude larger than that of fura-2.

In addition to the difference in rate constants, the higher K_d of furaptra for calcium weights the volume-averaged furaptra signal toward compartments closer to the voltage-dependent calcium channels, the site of calcium influx. It has been shown at the squid giant synapse (Smith et al., 1993) and with simulations (Sala and Hernandez-Cruz, 1990) that the evoked rise in $[Ca^{2+}]$ is fastest at intracellular compartments closest to the calcium channels. However, in a structure as small as the CA3-CA1 presynaptic terminals, this may not be a significant factor, because the characteristic time required for diffusion is very small. The characteristic time for a substance with diffusion coefficient D in a structure with radius r is equal to $r^2/6D$ (Crank, 1978). Assuming that the effective diffusion coefficient of Ca^{2+} was 10^{-7} cm^2/s because of binding to buffers, Regehr and Alturi (1995) calculated that the characteristic time for a 1 μm structure would be only 4 ms. Because our simulations indicate that the predominant calcium buffers in CA3-CA1 presynaptic terminals are relatively slow, the effective diffusion coefficient will not be as small as assumed by Regehr and Alturi (1995); therefore, the characteristic time required for diffusion across these terminals will be even smaller than 4 ms.

The rapid rising phase of the furaptra transient is similar to that of the presynaptic $[Ca^{2+}]_t$ evoked by a single action potential at the squid giant synapse, as recorded with the calcium indicator arsenazo III, which rises to the peak within 1–2 ms and remains above resting levels for about 10 s (Charlton et al., 1982). The rapid rising phase with the resultant short duration of the volume-averaged calcium influx provides an upper limit (~2 ms) for the duration of the presynaptic calcium influx evoked by a single action potential at hippocampal CA3-CA1 synapses. This is only an approximation, because the time constant of the rising phase of the furaptra transient is dependent on the actual amplitude of the calcium influx. As discussed above, diffusion and endogenous buffers can also affect this time course; however, their effect is likely to be relatively small in these presynaptic terminals. These results are in good agreement with the duration of I_{Ca} recorded from the calyx of Held, a large presynaptic terminal located in the medial nucleus of the trapezoid body (MNTB), in response to an action potential (Borst and Sakmann, 1996), and from the somata of cultured rat cerebellar granule cells in response to a mock action potential (Wheeler et al., 1996). In the latter paper, the potassium channel blocker 4-aminopyridine was observed to broaden the presynaptic action potential and prolong the duration of I_{Ca}. In agreement with our interpretation that the duration of the volume-averaged calcium influx approximates the duration of I_{Ca}, we observed that application of 4-aminopyridine increased the duration of the volume-averaged calcium influx (unpublished observation). Recently, similar fast-rising calcium transients were recorded from single presynaptic terminals of cultured rat cortical neurons (Mackenzie et al., 1996).

Characteristics of intrinsic buffers

Adjusting parameters in the model presynaptic terminal to fit the time course of the decay phase of the furaptra transients indicated that the predominant endogenous buffer in these terminals is likely to be relatively slow. Although it was possible to obtain the observed decay $\tau_{1/2}$ of 30 ms by varying several parameters, a predominant endogenous buffer that is slow appears to be the most likely. Altering the properties of the fast, mobile endogenous buffer, B_1, was not sufficient to slow the decay of the modeled furaptra transient to the experimentally observed values (Fig. 5 *A*). Only when the properties were altered to an extent where B_1 did not play a significant role in shaping the calcium transient or when parameters (e.g., K_d) were adjusted to values well outside the range determined in other preparations, did the modeled $\tau_{1/2}$ even approach the experimental value. The K_d of B_1 necessary to model the experimental $\tau_{1/2}$ was >25 μM. Berlin et al. (1994) estimated K_d of the fast buffer to be approximately 0.96 μM in rat ventricular myocytes; Lagnado et al. (1992) estimated a K_d of 0.66 μM in rods from the salamander retina. Other groups have concluded that the K_d of the fast endogenous buffer must be greater than 1 μM, based on the observation that the differential calcium binding ratio (κ_B; see Eq. 8) does not change significantly for $[Ca^{2+}]$ up to 1 μM in various preparations: bovine adrenal chromaffin cells (Neher and Augustine, 1992; Zhou and Neher, 1993), the axons of *M. infundibulum* (Al-Baldawi and Abercrombie, 1995), and pituitary melanotrophs (Thomas et al., 1990). Based on these data, it seems unlikely that the K_d of B_1 in mammalian presynaptic terminals is >25 μM, as would be necessary to reproduce the experimental data. The kinetic parameters of the calcium indicators have been determined accurately in vitro. Some experiments have suggested that these parameters may be somewhat different in certain tissues (Baylor and Hollingworth, 1988); however, the differences are highly unlikely to be as large as would be needed to match the experimental

$\tau_{1/2}$ (Fig. 5 *B*). The indicator concentration is the most uncertain indicator parameter; however, based on the observation that loading the slice with either fura-2 or furaptra did not significantly alter synaptic transmission, we believe the concentration is less than 10 μM (Fig. 5 *C*).

Removing the fast buffer B_1 from the simulation and reducing the k_{on} of the slow endogenous buffer, B_2, to 5×10^4 or 2×10^4/M·s gave half-decay times of 21 or 33 ms, respectively (Fig. 6 *A*). Decreasing $[B_2]$ or increasing its K_d by an order of magnitude would also give approximately correct values for $\tau_{1/2}$. However, we chose to alter the k_{on} for two reasons. First, $[B_2]$ and K_d are inherently simpler to determine than the kinetic parameter, k_{on}; therefore, $[B_2]$ and K_d values are less likely to be in error. Second, the required changes in $[B_2]$ or K_d would both reduce the differential calcium-binding ratio, κ_B, below the range of values observed in various neuronal preparations (Eq. 8; Neher, 1995).

Based on the above reasoning, we concluded that the predominant endogenous buffer is likely to be relatively slow with the following approximate characteristics: [B] = 600 μM, K_d = 400 nM, and $k_{on} = 5 \times 10^4$/M·s. In the simulations presented in this paper, this buffer was set to be immobile; however, this is not critical, as diffusion has little effect on the results of this model. No experimental data are available as to the characteristics of the endogenous buffers in this preparation; however, there is some indication that the buffering capacity of mammalian CNS presynaptic terminals may be relatively low and slow compared to invertebrate preparations. Directly recording from the large presynaptic terminals, the calyces of Held, in the medial nucleus of the trapezoid body (MNTB) in rat brain slices, showed that the endogenous mobile buffer capacity was relatively low (Borst et al., 1995). In this terminal, less than 50 μM BAPTA was needed to mimic the endogenous mobile buffer. Using the techniques reviewed by Neher (1995), the calcium binding ratio of the endogenous buffer (κ_B) in these terminals appears to be relatively low compared to most preparations (F. Helmchen, personal communication). In contrast to this low capacity, in frog saccular hair cells, the endogenous mobile buffer capacity is equivalent to approximately 800 μM BAPTA (Roberts, 1993); the mobile buffering capacity in presynaptic terminals of the squid giant synapse is also likely to be relatively high (Adler et al., 1991). Although the slow buffer in our simulations was based on intracellular calcium stores such as the smooth endoplasmic reticulum (Sala and Hernandez-Cruz, 1990), neither the experimental data nor the model allows us to comment on the exact nature of the endogenous buffers beyond the fact that the predominant buffer is relatively slow, with the approximate characteristics indicated above. Our results do not exclude the presence of a small amount of fast endogenous buffer; they indicate only that it is not the predominant buffer present in these terminals.

It should be noted that smooth endoplasmic reticulum is present in axons and presynaptic terminals in the mammalian nervous system (Peters et al., 1991). However, the predominant buffer may not be the smooth endoplasmic reticulum. In fact, this buffer may even be a mobile buffer, as buffer mobility produces only very minor effects in our model. Last, various other calcium buffers that are less important in shaping the single action potential evoked presynaptic calcium transient may be present and important for shaping calcium transients of different time scales or amplitudes.

Relationship between presynaptic Ca^{2+} and transmitter release

Using the nonspecific VDCC blocker Cd^{2+}, we determined the relationship between the transmitter release and presynaptic $[Ca^{2+}]_t$ or calcium influx (Figs. 8 and 9). Both relationships could be described by a power law (Eq. 1) with exponents of approximately 4 ($m \approx 4$). This is the same result that we obtained previously using fura-2 at these synapses (Wu and Saggau, 1994a). Near the transmitter release sites, fura-2 is likely to be saturated by local high $[Ca^{2+}]$ responsible for triggering release, which is estimated to range from tens to hundreds of μM (Roberts et al., 1990; Llinás et al., 1992; Heidelberger et al., 1994). However, based on the present results, the fura-2 signal must still be proportional to the local high $[Ca^{2+}]$ and able to reflect relative changes. Because of the small size of these terminals, the volume-averaged $[Ca^{2+}]$ is proportional to the local high $[Ca^{2+}]$ concentration responsible for release. In a larger structure or one with significantly higher endogenous buffering capacity, the relationship between the volume-averaged $[Ca^{2+}]$ and the local $[Ca^{2+}]$ would be much more nonlinear. In this case, local saturation of fura-2 would be much more relevant to its utility in gauging the relationship between presynaptic calcium and transmitter release.

The other concern about using fura-2 to measure the relationship between presynaptic calcium and transmitter release is based on the observation that externally applied Cd^{2+} enters rat cerebellar parallel fiber terminals loaded with fura-2 and binds to the indicator (Regehr and Alturi, 1995). This reduces the fluorescence of the slice when excited at 380 nm (F) and will affect $\Delta F/F$. However, the expected effect on the amplitude of $\Delta F/F$ is relatively small. When excited at 380 nm, the fluorescence of free fura-2 is nearly 20-fold higher than bound fura-2; also, as noted previously, the off rate constant (k_{off}) of fura-2 is relatively small. The effect of Cd^{2+} will be to bind some of the fura-2; these molecules will make very little contribution to the resting fluorescence of the terminal. Because of their slow off rate, the fura-2 molecules will also make very little contribution to the rising phase of the evoked transient. Thus the effect on the amplitude of $\Delta F/F$ will be very small. The expected direction of effect is to decrease the amplitude of $\Delta F/F$, because although the Cd^{2+}-bound fura-2 makes only a small contribution to F, it will make an even smaller contribution to ΔF. Therefore, Cd^{2+} binding to fura-2 would lead to an overestimation of the exponent in the

relationship between $\Delta F/F$ and transmitter release. The exponent measured with fura-2 was actually smaller than measured with furaptra, which does not seem to be affected by Cd^{2+} (Regehr and Alturi, 1995). This confirms that the effect of Cd^{2+} binding to fura-2 on the amplitude of the fura-2 transient is indeed very small. The largest effect of Cd^{2+} bound to fura-2 on $\Delta F/F$ would be during the decay phase of the transient. However, even this effect appears to be relatively small, because the shape of initial portion (25 ms) of the fura-2 transient was not altered by the bath application of Cd^{2+} (see Fig. 4 in Wu and Saggau, 1994a).

Thus both the results in the present study using furaptra and those of our past experiments using fura-2 indicate that transmitter release in guinea pig CA3-CA1 synapses is proportional to approximately the fourth power of presynaptic $[Ca^{2+}]$ or calcium influx. This was consistently the case for various manipulations that alter presynaptic calcium influx. These manipulations have included the application of nonspecific and specific blockers of VDCC: 1) Cd^{2+} (Fig. 9; Wu and Saggau, 1994a); 2) ω-CTx-GVIA (Wu and Saggau, 1994b); 3) ω-ATx-IVA (Wu and Saggau, 1994b); and 4) ω-CTx-MVIIC (Wu and Saggau, 1995a). Similar results were obtained during application of presynaptic modulators: agonists of adenosine A_1 receptors (Wu and Saggau, 1994c), $GABA_B$ receptor (Wu and Saggau, 1995b), and muscarinic receptors (Qian et al., 1995). This indicates that these modulators have their main effect on evoked transmitter release upstream of or at the level of the VDCCs. The same exponent has also been observed during manipulations that increased presynaptic calcium influx: altering extracellular $[Ca^{2+}]$ (unpublished data) and removing extracellular $[Mg^{2+}]$ (Fig. 3). Except for the work in this paper, all other results were obtained with fura-2; however, based on the work in this paper, we believe that the previous results were not affected by local fura-2 saturation or interaction with Cd^{2+}.

At the rat cerebellar parallel fiber to Purkinje cell synapse, the relationship between presynaptic calcium and transmitter release appears to be quite different. During the application of Cd^{2+} or ω-CTx-GVIA or during the application of salines with different extracellular $[Ca^{2+}]$, the exponent was approximately $m = 2.5$; the exponent was $m = 4$ during the application of ω-ATx-IVA (Mintz et al., 1995). The discrepancy was not a result of differences in indicators used, as furaptra was used for all experiments. They may be a result of differences in the species used or differences in the synapses under investigation. The different exponents obtained with different manipulations in the rat cerebellum may indicate that the ω-ATx-IVA-sensitive VDCCs are significantly closer to the release sites compared to other VDCCs, which would then be less effective in causing release. This distance has to be such that the relationship between the influx through a channel and the concentration achieved near the release site is nonlinear. A possible source of the nonlinearity would be binding to endogenous or exogenous calcium buffers. Thus the difference between the two synapses could be due to different patterns of localization of VDCCs, differences in endogenous buffering, or differences in the concentration of exogenous buffer achieved. It should be noted that the techniques used for selectively loading these presynaptic terminals were different (Regehr and Tank, 1991; Wu and Saggau, 1994a); this fact, in combination with the differences in preparations, could easily lead to very different concentrations of indicator in the presynaptic terminals.

I_{Ca} evoked by a single action potential

The fact that furaptra and fura-2 measurements gave similar values for the exponent relating presynaptic calcium and transmitter was used to determine an upper limit for I_{Ca} evoked by a single action potential. I_{Ca} must be small enough that the volume-averaged fura-2 transient is not saturated and is still able to reflect relative changes in local $[Ca^{2+}]$ near the release sites. Using the model parameters that were determined above, we estimated the upper limit to be approximately 1 pA for 1 ms. This value is highly dependent on [fura-2] in the terminal. Although we do not have a direct estimate of [fura-2], it is unlikely to be higher than 10 μM: our simulation results indicate that approximately 20 μM of even the low-affinity indicator furaptra, which has a much smaller effect on intracellular $[Ca^{2+}]$ than the higher-affinity indicator fura-2, would significantly reduce transmitter release from these terminals. Yet we did not observe such a reduction with either furaptra or fura-2. Further credence is lent to this estimate for [fura-2] by the observation that less than 50 μM BAPTA is sufficient to affect synaptic transmission at another mammalian synapse (Borst et al., 1995). Even if [fura-2] were as high as 50 μM, modeling results still indicate that a current of 5 pA would be sufficient to saturate fura-2. Moreover, even in the case in which a large quantity of fast endogenous buffer (e.g., "initial values" for buffer parameters) is present in the presynaptic terminal, saturation of fura-2 still occurs near 5 pA.

It should be noted that these values are also dependent on the duration of I_{Ca} used. More important than the amplitude or duration of I_{Ca} is the product of these two quantities, which reflects the number of Ca^{2+} ions that enter the terminal. For example, if the duration were halved, the amplitude could be roughly doubled without saturating the fura-2 signal. All simulations were performed for an I_{Ca} of 1 ms duration, because the upper limit for the duration was established as 2 ms, based on the furaptra transients. Assuming that under physiological conditions the single channel conductance of a VDCC is approximately 4 pS (Miller and Hu, 1995) and that the driving force is approximately 100 mV, on average only 2.5 channels would need to open to provide 1 pA of I_{Ca}. This estimates the lower limit of the number of VDCCs that open in a presynaptic terminal during an action potential. The total current is likely to be composed of channels opening at different times and for different durations. If, for example, each channel only

opened for a total of 200 μs, then 12.5 channels would need to open to obtain the equivalent of 1 pA for 1 ms. Of course, if the actual I_{Ca} is nearer to 5 pA, the number of open channels would be approximately fivefold greater. These estimates are for the number of channels that open after an action potential, not the total number of channels available at the presynaptic terminal.

Two recent studies have investigated calcium transients evoked by an action potential in single presynaptic terminals in cultured cortical neurons (Mackenzie et al., 1996) or neocortical pyramidal cells in brain slices (Svoboda et al., 1996). Both found that action potentials always led to calcium influx in presynaptic terminals; moreover, the trial-to-trial variability of amplitudes of the calcium transients was relatively small. Mackenzie et al. (1996) found the variability to be approximately 20% of the mean amplitude. Assuming a Poisson distribution, the number of VDCCs opening on an average trial would be 25. In contrast, based on the discussion above, we predict that only 5–10 VDCCs would open after an action potential. The discrepancy may be a result of the difference in preparations used. Another possibility is that because of the high concentration of fura-2 (750 μM in the whole-cell recording pipette) used by Mackenzie et al. (1996), they may have underestimated the degree of variability in the calcium transients. Although the actual concentration in the terminals is undoubtedly smaller than the concentration in the pipette, it may still be sufficient to reduce the trial-to-trial variability. The variability that would be observed for 5 or 10 channels opening is only 45% or 32%, respectively.

CONCLUSION

Based on imaging of presynaptic calcium transients using calcium indicators with different affinities for calcium and on modeling of these transients, we were able to draw several conclusions about calcium dynamics in mammalian presynaptic terminals and about the use of calcium indicators for measuring these properties. We have shown that both fura-2 and furaptra are capable of accurately measuring the nonlinear relationship between presynaptic calcium and transmitter release. At hippocampal CA3 to CA1 pyramidal cell synapses, transmitter release is approximately proportional to the fourth power of the calcium concentration or influx. The calcium influx evoked by an action potential in these terminals is small (~1 pA), is of brief duration (<2 ms), and most likely involves the opening of very few VDCCs (5–10). Last, although small quantities of a fast calcium buffer may be present, the predominant calcium buffer in these presynaptic terminals is relatively slow and may correspond to the smooth endoplasmic reticulum.

We would like to thank E. P. Cook, J. Qian, and E. D. Roberson and Drs. C. M. Colbert, S. S. Patel, and J. D. Sweatt for critical and helpful comments on this manuscript. The data collection software was written by Dr. S. S. Patel.

This work was supported by National Institutes of Health grant NS33147 to PS and NIMH grant MH10491 to SRS.

REFERENCES

Adler, E. M., G. J. Augustine, S. N. Duffy, and M. P. Charlton. 1991. Alien intracellular calcium chelators attenuate neurotransmitter release at the squid giant synapse. *J. Neurosci.* 11:1496–1507.

Al-Baldawi, N. F., and R. F. Abercrombie. 1995. Cytoplasmic calcium buffer capacity determined with Nitr-5 and DM-nitrophen. *Cell Calcium.* 17:409–421.

Andersen, P. 1975. Organization of hippocampal neurons and their interconnections. *In* The Hippocampus. Vol. 1: Structure and Development. R. L. Isaacson and K. H. Pribram, editors. New York: Plenum Press. 155–175.

Augustine, G. J., E. M. Adler, and M. P. Charlton. 1991. The calcium signal for transmitter secretion from presynaptic nerve terminals. *Ann. N.Y. Acad. Sci.* 635:365–381.

Augustine, G. J., and M. P. Charlton. 1986. Calcium dependence of presynaptic calcium current and post-synaptic response at the squid giant synapse. *J. Physiol. (Lond.).* 381:619–640.

Augustine, G. J., M. P. Charlton, and S. J. Smith. 1985. Calcium entry and transmitter release at voltage-clamped nerve terminals of squid. *J. Physiol. (Lond.).* 369:163–181.

Baylor, S. M., and S. Hollingworth. 1988. Fura-2 calcium transients in frog skeletal muscle fibers. *J. Physiol. (Lond.).* 403:151–192.

Berlin, J. R., J. W. M. Bassani, and D. M. Bers. 1994. Intrinsic cytosolic calcium buffering properties of single rat cardiac myocytes. *Biophys. J.* 67:1775–1787.

Berlin, J. R., and M. Konishi. 1993. Ca^{2+} transients in cardiac myocytes measured with high and low affinity Ca^{2+} indicators. *Biophys. J.* 65: 1632–1647.

Borst, J. G. G., F. Helmchen, and B. Sakmann. 1995. Pre- and postsynaptic whole-cell recording in the medial nucleus of the trapezoid body of the rat. *J. Physiol. (Lond.).* 489:825–840.

Borst, J. G. G., and B. Sakmann. 1996. Calcium influx and transmitter release in a fast CNS synapse. *Nature.* 383:431–434.

Charlton, M. P., S. J. Smith, and R. S. Zucker. 1982. Role of presynaptic calcium ions and channels in synaptic facilitation and depression at the squid giant synapse. *J. Physiol. (Lond.).* 323:173–193.

Clements, J. D., R. A. J. Lester, G. Tong, C. E. Jahr, and G. L. Westbrook. 1992. The time course of glutamate in the synaptic cleft. *Science.* 258:1498–1501.

Cohen, M. W., O. T. Jones, and K. J. Angelides. 1991. Distribution of Ca^{2+} channels on frog motor nerve terminals revealed by fluorescent ω-conotoxin. *J. Neurosci.* 11:1032–1039.

Crank, J. 1978. *The Mathematics of Diffussion*, 2nd ed. Clarendon Press, Oxford.

Dittman, J. S., and W. G. Regehr. 1996. Contributions of calcium-dependent and calcium-independent mechanisms to presynaptic inhibition at a cerebellar synapse. *J. Neurosci.* 16:1623–1633.

Dodge, F. A., and R. Rahamimoff. 1967. Co-operative action of calcium ions in transmitter release at the neuromuscular junction. *J. Physiol. (Lond.).* 193:419–432.

Grynkiewicz, G., M. Poenie, and R. Y. Tsien. 1985. A new generation of Ca^{2+} indicators with greatly improved fluorescence properties. *J. Biol. Chem.* 260:3440–3450.

Heidelberger, R., C. Heinemann, E. Neher, and G. Matthews. 1994. Calcium dependence of the rate of exocytosis in a synaptic terminal. *Nature.* 371:513–515.

Kao, J. P. Y., and R. Y. Tsien. 1988. Ca^{2+} binding kinetics of fura-2 and azo-1 from temperature-jump relaxation measurements. *Biophys. J.* 53: 635–639.

Katz, B., and R. Miledi. 1970. Further study of the role of calcium in synaptic transmission. *J. Physiol. (Lond.).* 207:789–801.

Konishi, M., and J. R. Berlin. 1993. Ca transients in cardiac myocytes measured with a low affinity fluorescent indicator, furaptra. *Biophys. J.* 64:1331–1343.

Lagnado, L., L. Cervetto, and P. A. McNaughton. 1992. Calcium homeostasis in the outer segments of retinal rods from the tiger salamander. *J. Physiol, (Lond.).* 455:111–142.

Landò, L., and R. S. Zucker. 1994. Ca^{2+} cooperativity in neurosecretion measured using photolabile Ca^{2+} chelators. *J. Neurophysiol.* 72: 825–830.

Llinás, R. R., M. Sugimori, and R. B. Silver. 1992. Microdomains of high calcium concentration in a presynaptic terminal. *Science.* 256:677–679.

Mackenzie, P. J., M. Umemiya, and T. H. Murphy. 1996. Ca^{2+} imaging of CNS axons in culture indicates reliable coupling between single action potentials and distal functional release sites. *Neuron.* 16:783–795.

Miller, A., and B. Hu. 1995. A molecular model of low-voltage-activated calcium conductance. *J. Neurophysiol.* 73:2349–2356.

Mintz, I. M., B. L. Sabatini, and W. G. Regehr. 1995. Calcium control of transmitter release at a cerebellar synapse. *Neuron.* 15:675–688.

Neher, E. 1995. The use of fura-2 for estimating Ca buffers and Ca fluxes. *Neuropharmacology.* 34:1423–1442.

Neher, E., and G. J. Augustine. 1992. Calcium gradients and buffers in bovine chromaffin cells. *J. Physiol. (Lond.).* 450:273–301.

Peters, A., S. L. Palay, and H. deF. Webster. 1991. The Fine Structure of the Nervous System: Neurons and Their Supporting Cells, 3rd Ed. Oxford University Press, New York.

Qian, J., L.-G. Wu, and P. Saggau. 1995. Presynaptic calcium influx is modulated during muscarinic receptor-induced presynaptic inhibition and LTP at CA3-CA1 synapses in guinea pig hippocampus. *Soc. Neurosci. Abstr.* 21:432.19.

Raju, B., E. Murphy, L. A. Levy, R. D. Hall, and R. E. London. 1989. A fluorescent indicator for measuring cytosolic free magnesium. *Am. J. Physiol.* 256:C540–C548.

Regehr, W. G., and P. P. Alturi. 1995. Calcium transients in cerebellar granule cell presynaptic terminals. *Biophys. J.* 68:2156–2170.

Regehr, W. G., K. R. Delaney, and D. W. Tank. 1994. The role of presynaptic calcium in short-term enhancement at the hippocampal mossy fiber synapse. *J. Neurosci.* 14:523–537.

Regehr, W. G., and D. W. Tank. 1991. Selective fura-2 loading of presynaptic terminals and nerve cell processes by local perfusion in brain slice. *J. Neurosci. Methods.* 37:111–119.

Roberts, W. M. 1993. Spatial calcium buffering in saccular hair cells. *Nature.* 363:74–76.

Roberts, W. M., R. A. Jacobs, and A. J. Hudspeth. 1990. Colocalization of ion channels involved in frequency selectivity and synaptic transmission at presynaptic active zones of hair cell. *J. Neurosci.* 10:3664–3684.

Robitaille, R., E. M. Adler, and M. P. Charlton. 1990. Strategic location of calcium channels at transmitter release sites of frog neuromuscular junction. *Neuron.* 5:773–779.

Saggau, P., L.-G. Wu, and I. Yehezkely. 1992. Optical recording of transients of cytosolic free calcium in synaptic structures of hippocampal CA1 pyramidal cells employing a novel selective loading technique in brain slices. *Biophys. J.* 61:2941.

Sala, F., and A. Hernandez-Cruz. 1990. Calcium diffusion modeling in a spherical neuron: relevance of buffering properties. *Biophys. J.* 57: 313–324.

Sinha, S. R., L.-G. Wu, and P. Saggau. 1996. A model of presynaptic calcium transients and neurotransmitter release from terminals in the mammalian central nervous system. *Biophys. J.* 70:A197.

Smith, S. J., J. Buchanan, L. R. Osses, M. P. Charlton, and G. J. Augustine. 1993. The spatial distribution of calcium signals in squid presynaptic terminals. *J. Physiol. (Lond.).* 472:573–593.

Stanley, E. F. 1993. Single calcium channels and acetylcholine release at a presynaptic nerve terminal. *Neuron.* 11:1007–1011.

Svoboda, K., D. W. Tank, and W. Denk. 1996. Action potential evoked calcium transients in individual neocortical presynaptic terminals measured using two photon fluorescence scanning microscopy. *Biophys. J.* 70:A371.

Thomas, P., A. Supernant, and W. Almers. 1990. Cytosolic Ca^{2+}, exocytosis, endocytosis in single melanotrophs of the rat pituitary. *Neuron.* 5:723–733.

Westrum, L. E., and T. W. Blackstad. 1962. An electron microscopic study of the stratum radiatum of the rat hippocampus (regio superior, CA1) with particular emphasis on synaptology. *J. Comp. Neurol.* 119: 281–309.

Wheeler, D. B., A. Randall, and R. W. Tsien. 1996. Changes in action potential duration alter reliance of excitatory synaptic transmission on multiple types of Ca^{2+} channels in rat hippocampus. *J. Neurosci.* 16: 2226–2237.

Wu, L.-G., and P. Saggau. 1994a. Presynaptic calcium is increased during normal synaptic transmission and paired-pulse facilitation, but not in long-term potentiation in area CA1 of hippocampus. *J. Neurosci.* 14: 645–654.

Wu, L.-G., and P. Saggau. 1994b. Pharmacological identification of two types of presynaptic voltage-dependent calcium channels at CA3-CA1 synapses of the hippocampus. *J. Neurosci.* 14:5613–5622.

Wu, L.-G., and P. Saggau. 1994c. Adenosine inhibits evoked synaptic transmission primarily by reducing presynaptic calcium influx in area CA1 of hippocampus. *Neuron.* 12:1139–1148.

Wu, L.-G., and P. Saggau. 1995a. Block of multiple presynaptic calcium channel types by ω-conotoxin-MVIIC at hippocampal CA3 to CA1 synapses. *J. Neurophysiol.* 73:1965–1972.

Wu, L.-G., and P. Saggau. 1995b. $GABA_B$ receptor-mediated presynaptic inhibition in guinea-pig hippocampus is caused by reduction of presynaptic Ca^{2+} influx. *J. Physiol. (Lond.).* 485:649–657.

Yawo, H., and N. Chuhma. 1994. ω-Conotoxin-sensitive and -resistant transmitter release from the chick ciliary presynaptic terminal. *J. Physiol. (Lond.).* 477:437–448.

Zhou, Z. and E. Neher. 1993. Mobile and immobile calcium buffers in bovine adrenal chromaffin cells. *J. Physiol. (Lond.).* 469:245–273.

Zucker, R. S., K. R. Delaney, R. Mulkey, and D. W. Tank. 1991. Presynaptic calcium in transmitter release and posttetanic potentiation. *Ann. N.Y. Acad. Sci.* 635:191–207.

Zucker, R. S., and A. L. Fogelson. 1986. Relationship between transmitter release and presynaptic calcium influx when calcium enters through discrete channels. *Proc. Natl. Acad. Sci. USA.* 83:3032–3036.